WESTERN INSTITUTE OF TECHNOLOGY AND HIGHER EDUCATION

Nanomaterials Engineering II

Autumn 2019

Activity 4

MEASUREMENT OF OXIDE LAYER

"Team C"

Erick Saúl Aranda González NT694722
Elaine Chavira Trejo NT697708
Daniel Hernández Mota NT702357
Samuel de Jesús Terrazas Zaffa NT703798

Prof. Dr. Milton Oswaldo Vázquez Lepe

Tlaquepaque Jalisco
Date: 04 November 2019

Abstract

Silicon wafer was submitted to thermal oxidation process (RTA) 9 min 14 seg at 800°C. That sample and subsequently were and characterized by XPS realizing measurement with angles of 5 to 55° to obtain information about the elemental composition, chemical bondings, and layer thickness.

Keywords: *Thermal oxidation, Si, XPS*

Introduction

In accordance with Deal and Grove (1965), for the formation of silicon dioxide layers by thermal oxidation of single-crystal silicon, the reported activation energies of rate constants vary between 27 and 100 kcal/mole for oxidation in dry oxygen and the oxidation proceeds by the inward movement of a species of oxidant rather than by the outward movement of silicon.

The transported species must go through the following stages:
1 It is transported from the bulk of the oxidizing gas to the outer surface where it reacts or is absorbed.
2 It is transported across the oxide film towards the silicon.
3 It reacts at the silicon surface to form a new layer of SiO_2.

The ratio of the growth of the oxide layer with respect to the oxidation time of silicon at a constant pressure of 760 Torr is presented in the next graphic [2].

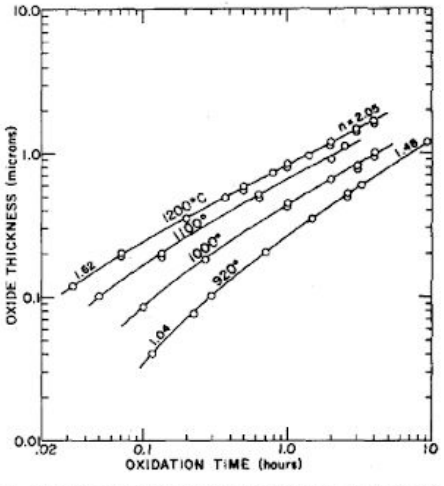

Figure. 1: Oxidation of silicon in dry oxygen at 760 Torr.

The flux of oxidation is the number of oxidant molecules crossing a unit surface area in a unit time. It is considered that the flux of gas oxidation to the vicinity of the outer surface (F_1) is:

$$F_1 = h\,(C^* - C_0)$$

Were:
h: gas-phase transport coefficient.
C_0: concentration of the oxidant at the outer surface of the oxide at any given time.
C*: equilibrium concentration of the oxidant in the oxide.

The equilibrium concentration of the oxidant is assumed to be related to the partial pressure of the oxidant in the gas by Henry's law and the oxidant is assumed to be molecular O_2, and H_2O for dry- and wet-oxygen oxidation, respectively. The figure 2, present a graph model for the oxidation of silicon, where X_o is a thick layer of oxide that covers the silicon [2].

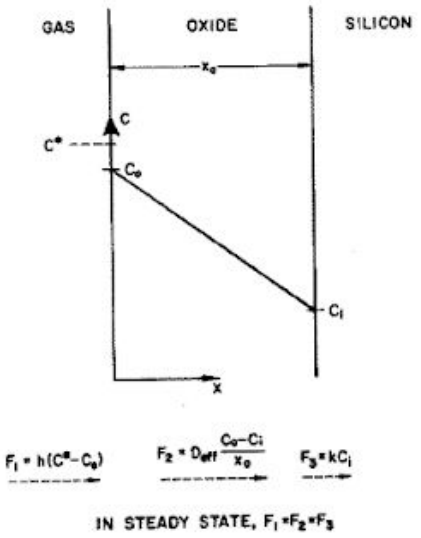

Figure 2. Model for the oxidation of silicon.

Have been demonstrated the selective surface enhancement that can be achieved in X-ray photoelectron spectroscopy (XPS) by utilizing low - or grazing - electron exit angles. Investigations have also suggested that surface layer thicknesses or electron attenuation lengths can be determined from quantitative analyses of angular-dependent peak intensities, provided that the effects of surface roughness are adequately allowed for [1].

Experimental procedure

During the experimental process the steps suggested in an oxidation by the RTA (Rapid Thermal Annealing) method were followed, adapting the equipment so that the oxidation process would be successful.

***Materials*:**
Quartz tube, Tubular Furnace (Thermo Scientific), Glass rod, Fan, see figure 3.

Figure 3: Materials. 1) Glass rod. 2) Quartz tube. 3) Fan. 4) Tubular Furnace (Thermo Scientific)

Reactives:
Isopropyl alcohol

Procedure:
The experimental procedure for proper oxidation consisted of the following steps.

1-The quartz was washed with isopropyl alcohol in order to have a clean surface of other elements that may influence the measurement.

2- Once the tube is clean, we proceed to insert the quartz tube into the tube furnace in order to start heating the tube to the desired temperature as shown in the Figure 4.

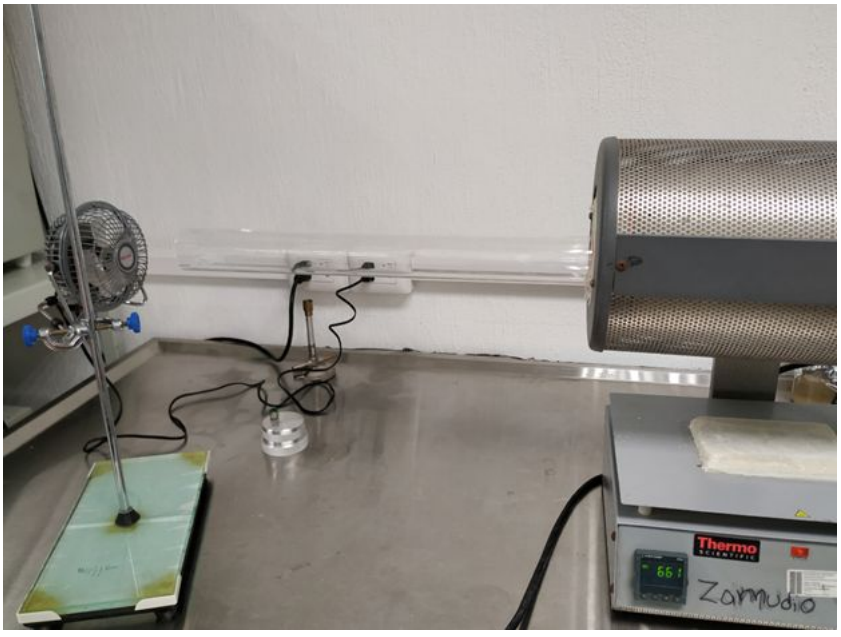

Figure 4: Structure of the experimental procedure.

3- Move the quartz tube a few centimetres out of the centre of the furnace to facilitate the process of introducing the sample.

4- Place the silicon wafer inside the quartz tube at one end with sterilized pliers, in order to avoid contamination of other elements in the sample, figure 5.

Figure 5: Quartz tube end wafer .

5-With the glass rod move the silicon wafer to the center of the tube (During this procedure you must be very careful to handle the rod, there is a risk of burning).

6-Once the silicon wafer is in the center of the tube, move the tube to the center of the tube furnace and at one end to introduce oxygen by means of a ventilated note: During this process great care must be taken because when the sample is in the center of the furnace, the oxidation time must begin to be measured accurately, Figure 6.

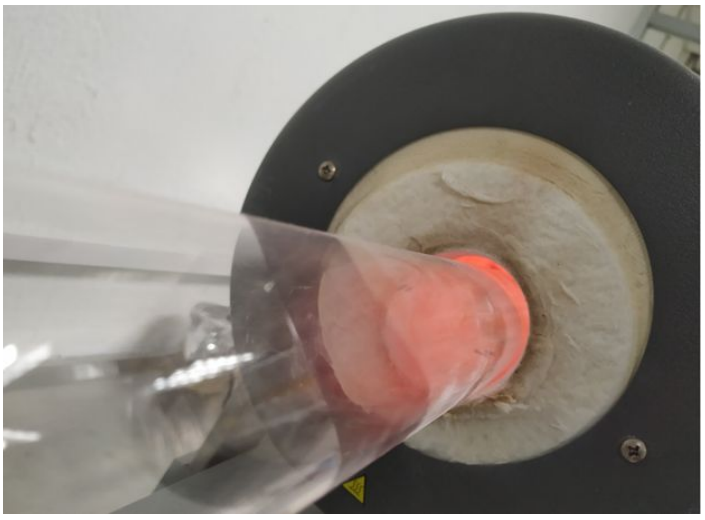

Figure 6: Silicon wafer in the center of the tube furnace in oxidation process.

7-Once the oxidation is finished, the sample is removed from the tube, moving the tube and pushing the silicon wafer with the glass rod outwards, allowing the wafer to cool to room temperature on the sample holder.

Characterization:

To obtain the chemical composition, the composition technique was used with XPS (SPECS). The conditions of these technique was registered in table 1.

Table 1: Conditions of the characterization techniques.

XPS	Pressure of the Analysis chamber	1.69E-9 mbar
	Incident X-ray	Al K-Alpha = 1487 eV

Results and discussion

XPS

At the beginning, a survey on the sample was conducted by a regular XPS technique, this can be seen in figure 7.

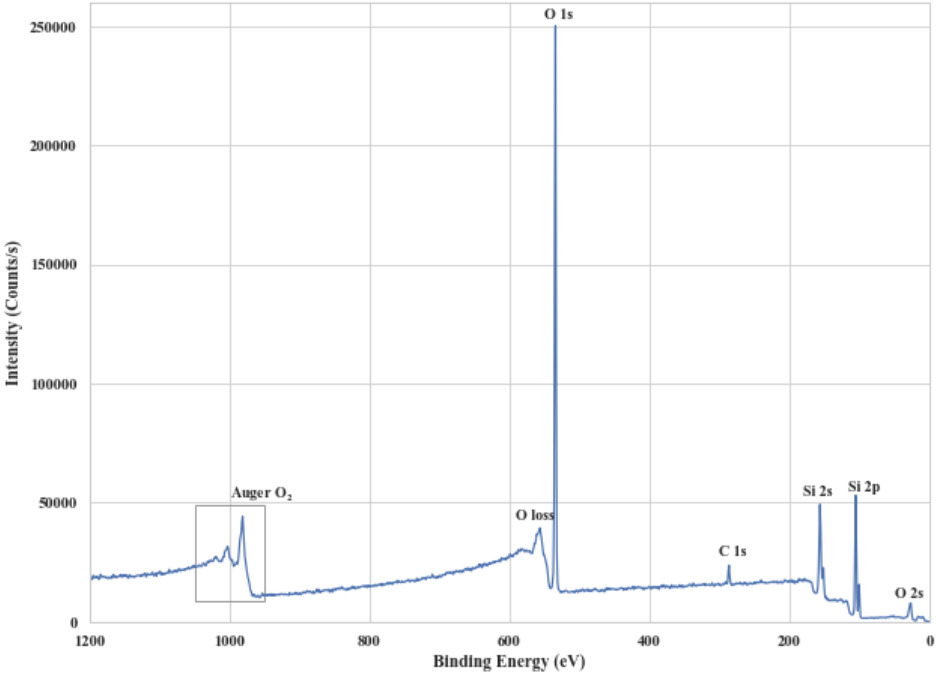

Figure 7: Survey of the sample.

Afterwards, an angular-dependent XPS technique was used to determine not only the chemical composition but the measurement of the width of oxidized silicon. A total of 6 measurements of 5, 15, 25, 35, 45 and 55 degrees were made to the sample in order to see the decrease on the intensity counts. The result of the chemical composition at 0° it can be observed at table 2, also we can observe in figure 7 the behaviour of the sample' chemical

composition, it can be notice that 28.35% of the Si 2p its bounded with oxygen.

Table 2: Chemical composition of the sample at 0°.

Core Level	Kinetic Energy (KE)	Binding Energy BE	Scofield Factor	Peak area (lij)	NI	% Atomic	% Atomic/Element
C 1s	1202.1	284.61	1	1068.14	7.46	3.86	C1s 3.86
O 1s	955.1	531.61	2.93	42650.50	119.40	61.72	O1s 61.75
Si 2p	1387.55	99.16	0.817	1317.68	10.19	5.27	Si 2p 34.39
Si (O_2) 2p	1382.61	104.1	0.817	6942.66	53.80	27.82	
Si (O_2) 2p	1384.67	102.04	0.817	132.20	1.02	0.53	
Si 2p	1387.08	99.63	0.817	193.29	1.49	0.77	
					185.91	100	100.00

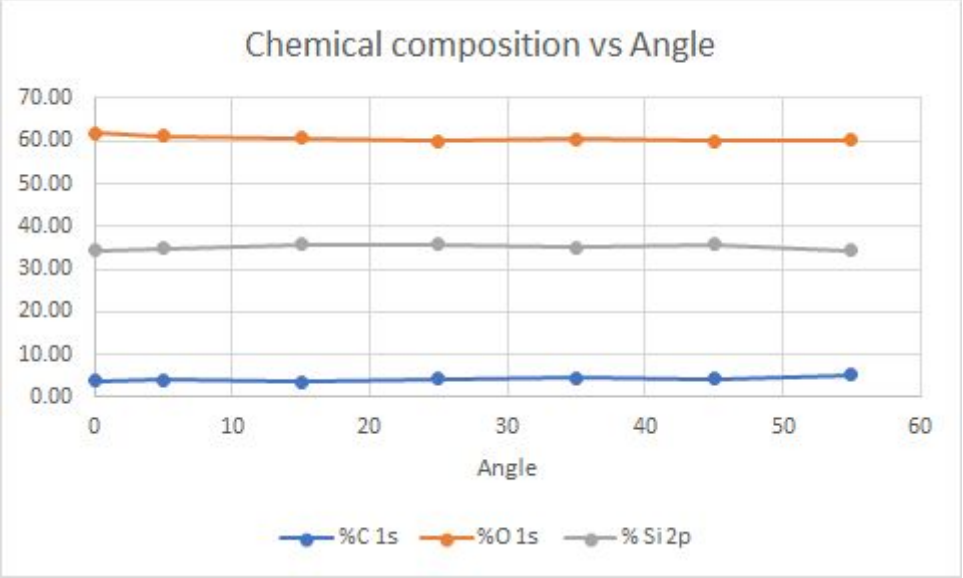

Figure 7: Chemical composition behaviour respect the angle of measurement.

It's important to mention that the XPS atomic percentage analysis was obtained based on the calculation of the peaks' areas that were obtained using *Aanalyzer* software. This mathematical procedure consists on applying the equations 1 and 2, to the table 2 data.

$$Ni = \frac{AREA(lij)}{(Scofield)x(KE)^{0.7}} \quad \text{Equation 1} \qquad \%Atom = \frac{(Ni)x(100)}{\sum Ni} \quad \text{Equation 2}$$

The peak areas were obtained from the high resolution peaks, same ones that we can see at the figure 8.The experimental data of the Si 2p peak, at each angle can be seen in figure 9.

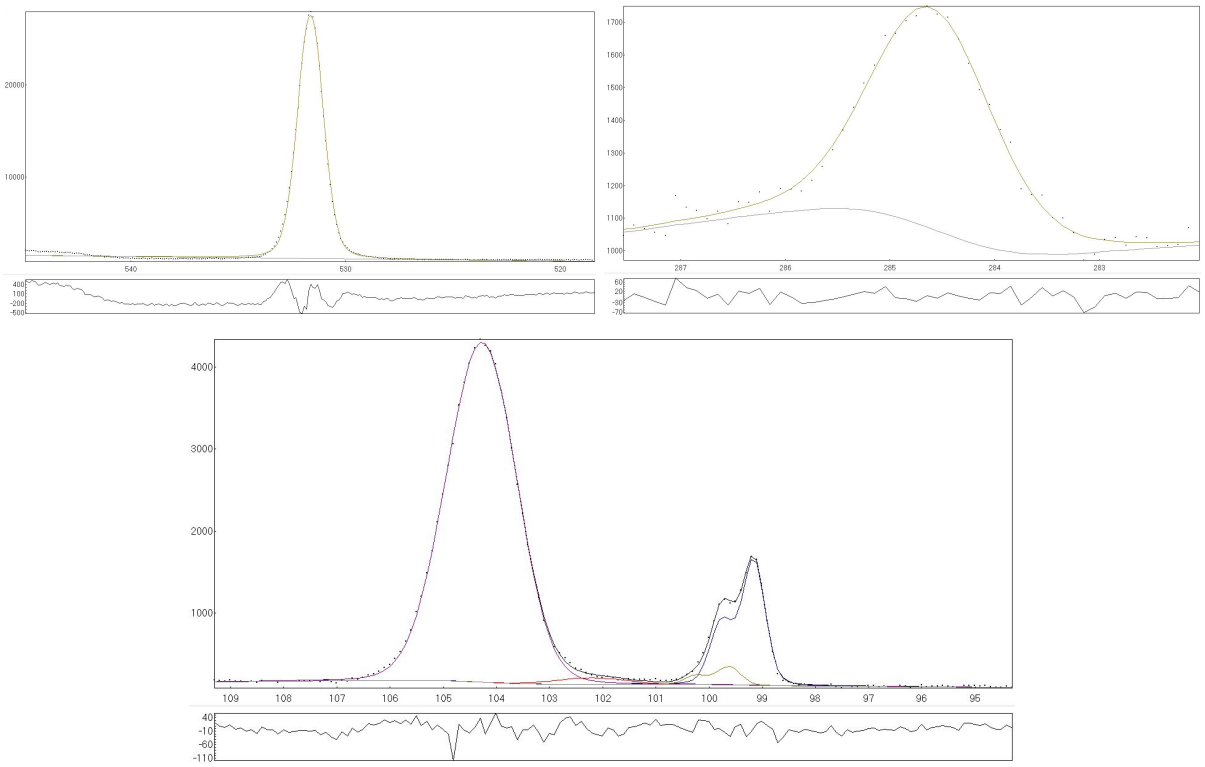

Figure 8: a) O 1s high definition peak (left), b) C 1s high definition peak (right) and c) Si 2p high definition peak (center), in this peak we can observe a little component (red one) that can be attributed to a Si semi-oxide. The colour peaks are generated when the *Aanalyzer* software calculates the area. The x axis referer to binding energy and the y axis to counts/second.

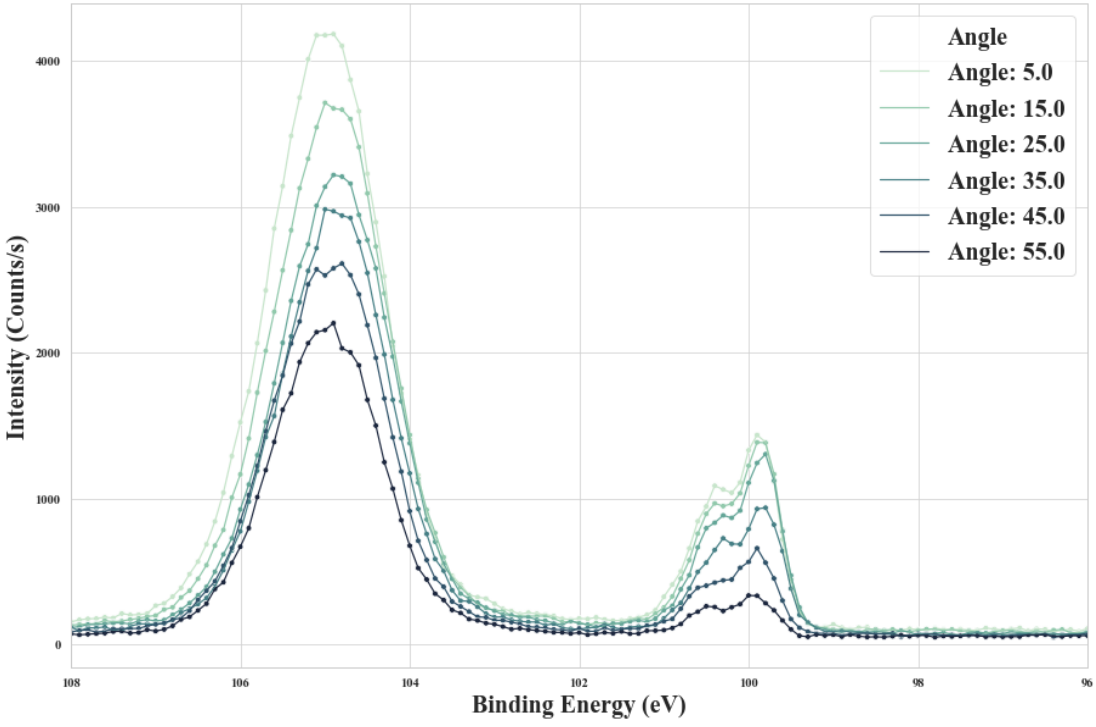

Figure 9: Angular measurements of the Si-SiO_2 experimental data. It is appreciable how the intensity decreases with an increase in the angle of the measurement.

The data was processed with the software *Aanalyzer*, where the experimental data was deconvoluted and fixed into a better representation of the samples. For the Silicon Oxide Intensity peak (generally centered at 104.5 on the Binding energy axis), two deconvolutions were made to represent correctly the data. Additionally, for the data of the elemental silicon (Si2p; mainly centered in 99.3), there were also two deconvolutions made. The fitted data can be seen in figure 10. A side by side comparison of the two graphs can be made, where it is possible to identify that the fitted data is more smooth than the raw experimental data.

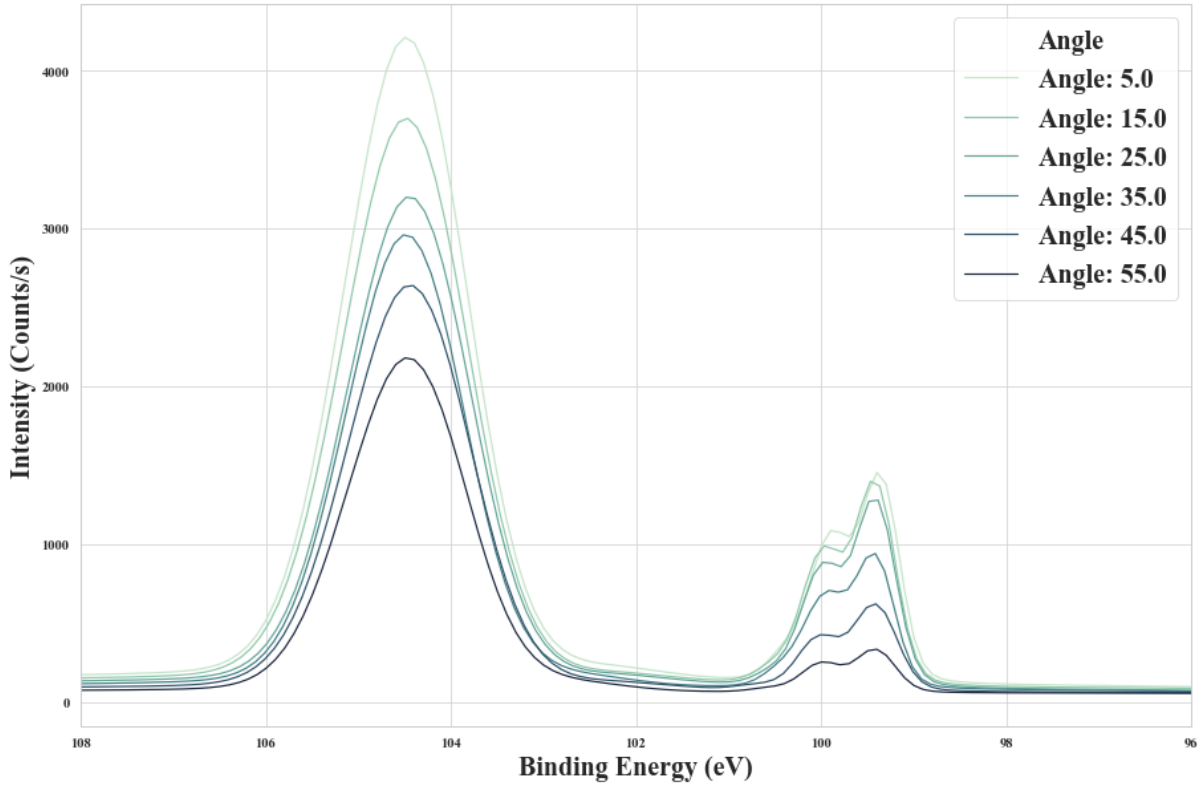

Figure 10: Fitted data for the angular dependence.

A 3D representation of figure 10 can also be made where there is another axis in which the angle can be supported. This can be seen in figure 11. It is worth mentioning that the complementary angles are just as equivalent as the usual angles, however, the function sine or cosine must be chosen wisely for the calculations. The relation can be seen in table 3.

Table 3: Expression of angles in degrees and radians with the complementary angle.

Angle (degrees)	Angle (radians)	Complementary Angle (degrees)	Complementary Angle (radians)
5	0.0872665	85	1.48353
15	0.261799	75	1.30900
25	0.436332	65	1.13446
35	0.610865	55	0.959931
45	0.785398	45	0.785398
55	0.959931	35	0.610865

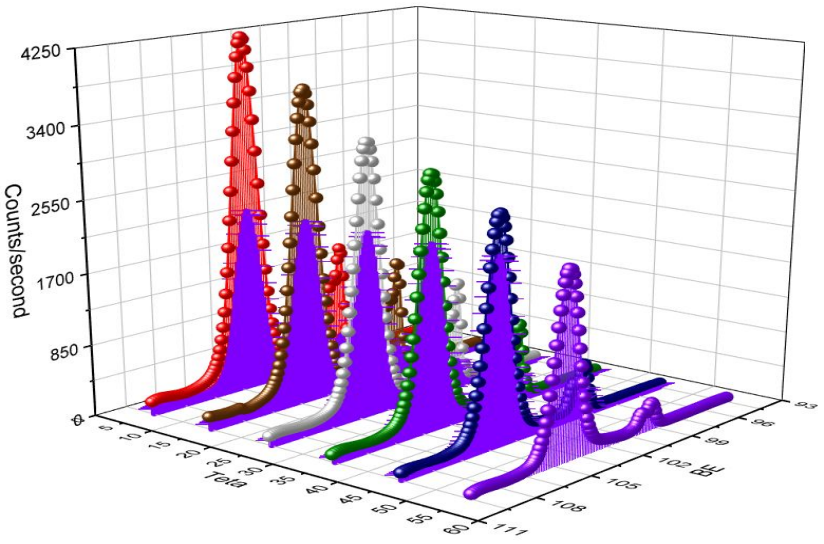

Figure 11: 3-D representation of the angular dependent measurements of the intensity of the fitted peaks.

The area of each peak was obtained based on the results from the *Aanalyzer* software. They were generally divided into the area of the elemental silicon (I_{Si}) and the area of the silicon dioxide (I_{SiO2}). The plotted areas can be seen in figure 12. It is obvious that the areas for I_{SiO2} are much higher than the ones on I_{Si} due to the intensity regarded in the graphs.

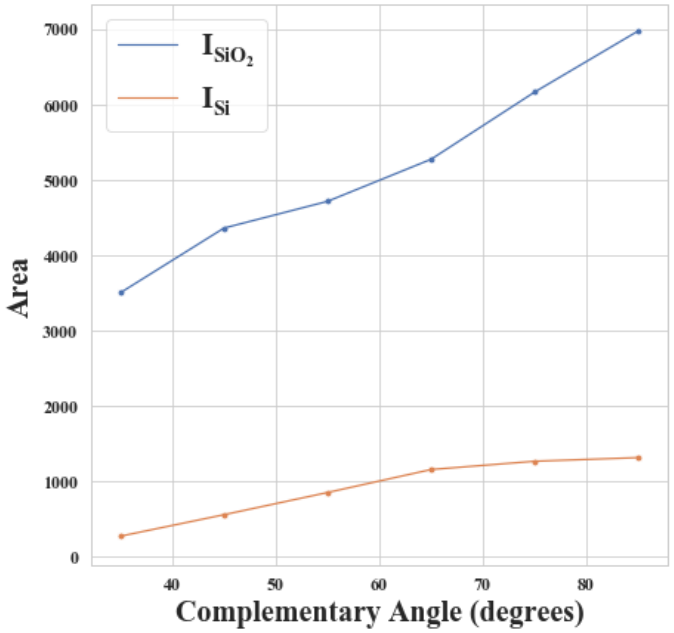

Figure 12: Areas from the peaks.

It is possible to determine a relation between areas. The formula to obtain this data is given by the equation:

$$R = I_{SiO_2} / I_{Si} \qquad \text{Equation 3}$$

By applying (3) to the results from figure 9, a graph can be generated (see figure 13).

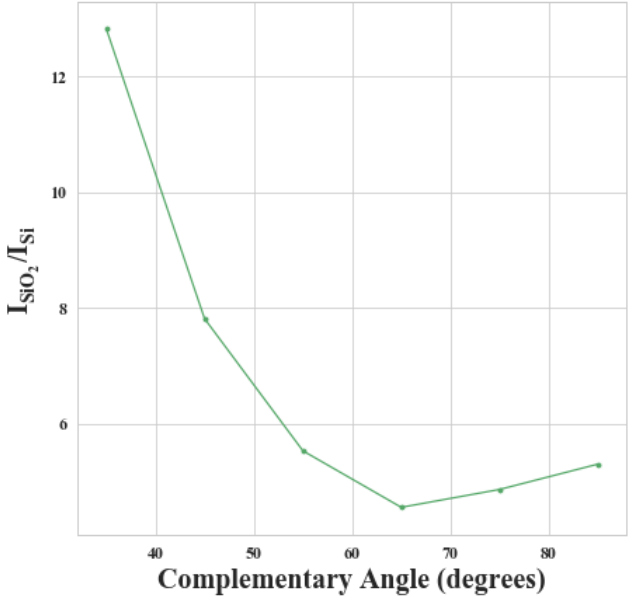

Figure 13. Relation between areas of Silicon Oxide and elemental silicon in the same sample with angle dependance.

All of the results that came from the *Analyzer* software and the relations between areas can be

seen in table 2. In the table peaks 0 and 1 belong to elemental silicon (Si2p) and peaks 1 and 3 belong to Silicon Oxide, therefore the areas for each peak (I_x) are composed by the sum of these peaks correspondingly.

Table 4: Results table from *Aanalyzer* containing the areas corresponding to each peak and their relation.

	Angle	Comp. Angle	Peak_0 (Si2p)	Peak_1 (SiO2)	Peak_2 (Si2p)	Peak_3 (SiO2)	Total Area	I Si_{2p}	I SiO_2	R
0	5.0	85.0	1039.40	6842.1	276.070	132.460	8290.011	1315.470	6974.560	5.301953
1	15.0	75.0	1094.80	6061.3	172.390	102.510	7431.037	1267.190	6163.810	4.864156
2	25.0	65.0	1019.30	5171.4	138.050	100.980	6429.677	1157.350	5272.380	4.555562
3	35.0	55.0	671.46	4609.1	180.960	105.350	5566.844	852.420	4714.450	5.530666
4	45.0	45.0	502.86	4280.2	55.238	79.527	4917.870	558.098	4359.727	7.811759
5	55.0	35.0	232.20	3411.3	40.984	90.664	3775.156	273.184	3501.964	12.819067

Measurements of completely oxidized silicon (figure 14) and elemental silicon (figure 15) were also done at the same angles to obtain a comparison and a relation between quantities to finally compute the thickness of the oxide layer.

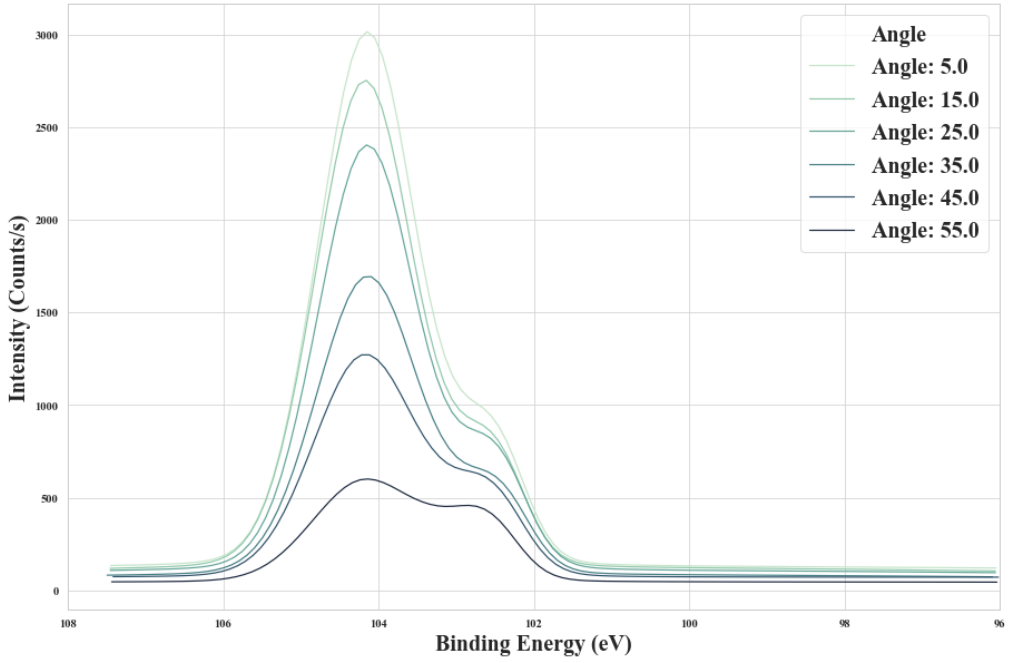

Figure 14: Measurements and fit of the graphs that represent a completely oxidized silicon sample with angle dependance.

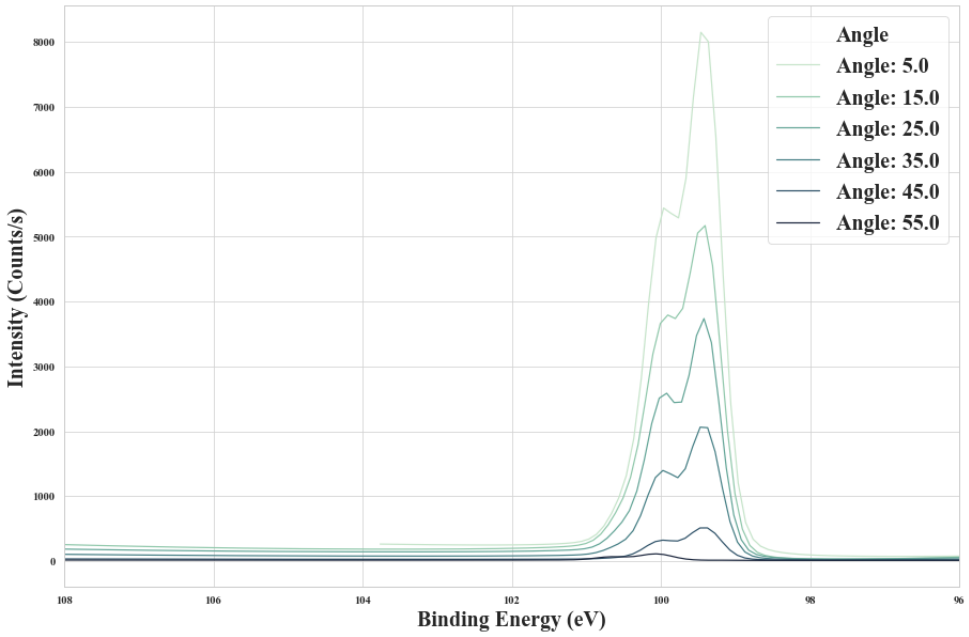

Figure 15: Measurements and fit of the graphs that represent a pure elemental silicon sample with angle dependance.

The same analysis of the areas from each peak can be applied to these separated measurements and also a relation of areas can be obtained, however the notation for this analysis changes. For each peak, a deconvolution was made including two correlated components, which yielded correctly the from of the spectrum analyzed.

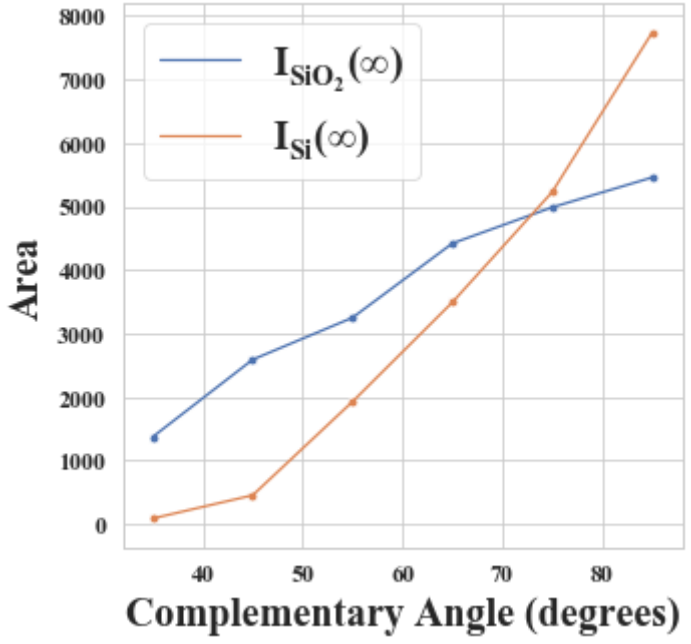

Figure 16. Areas for the peaks of silicon and silicon dioxide from the figures 9 and 10.

In this case, since an analysis for a completely oxidized silicon specimen and a pure elemental sample are being measured, a relation of areas can be obtained given by the equation 4. The graphical representation can be observed in figure 17.

$$K = I_{SiO_2}(\infty) / I_{Si}(\infty) \tag{4}$$

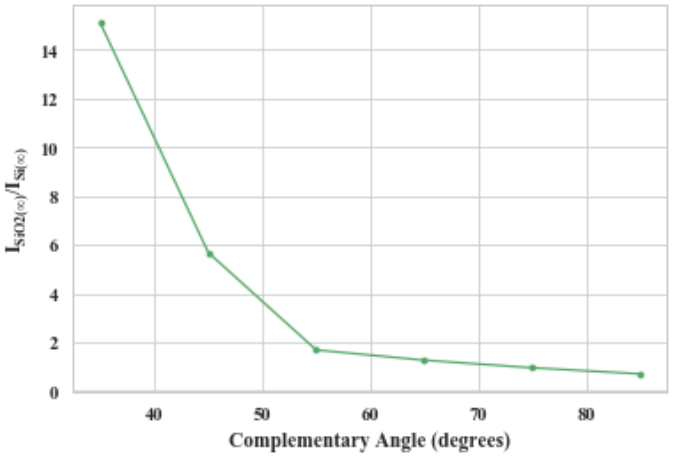

Figure 17. Relation between areas of a completely oxidized silicon and a pure elemental silicon in different samples with an angle dependance.

With this information it is possible to obtain the thickness of the oxide layer. To do this equation 5 must be used as a linear relation between all the combined data.

$$ln\,(1 + R/K) \;=\; 1/sin(\theta)\;\; d/\lambda \tag{5}$$

where ln is the natural logarithm, R and K are equations (4) and (5) respectively, θ is the angle of measurement (if complementary angle is used, then cosine of θ should be applied), d is the thickness of the oxide layer and λ is the mean free path.

In this case, to generate the linear relation, a substitutions of variables must be done:

$$y = ln\,(1 + R/K) \tag{6}$$
$$x = \;1/sin(\theta) \tag{7}$$
$$m \;=\; d/\lambda \tag{8}$$

thus the final (linearized) equation is:

$$y = x\,m \tag{9}$$

By plotting the data using (5) and then applying a linear regression with the data, we obtain different linear graphs depending on the number of values used for the linear regression (figure 18).

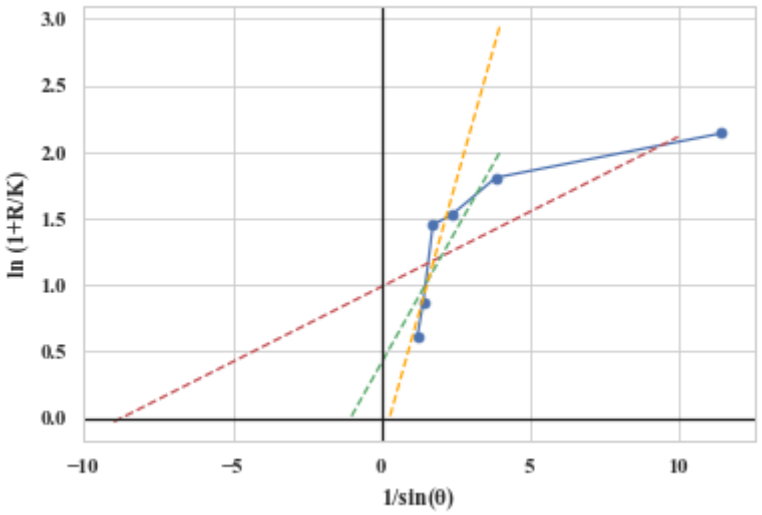

Figure 18: Plotted data and with the corresponding linear regressions

In this figure, the red line considers all of the points for the linear regression model, the green line considers one less point and the orange line considers two less points. It is possible to see that the line that best approaches "0" for an application of (9) is the orange linear regression, thus we will stick to that model (figure 19).

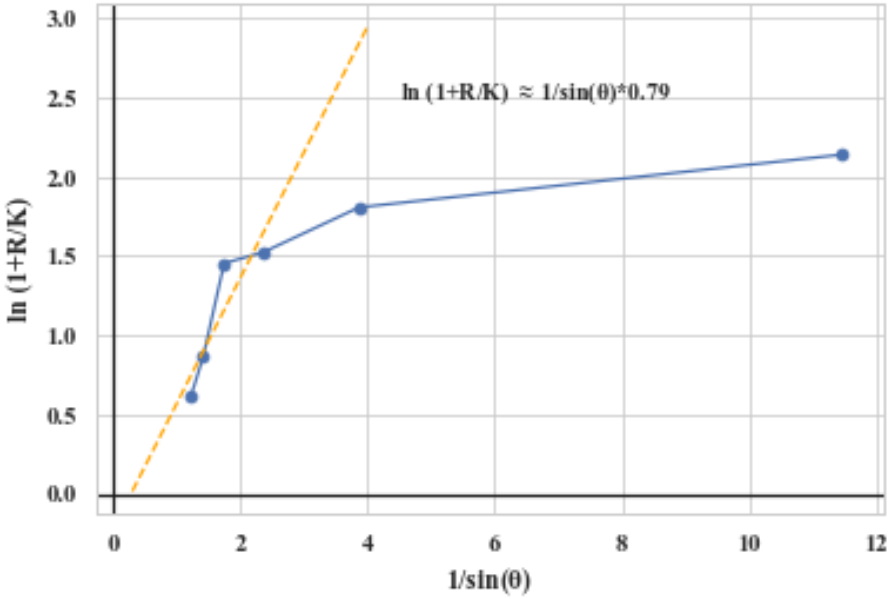

Figure 19: Best fit for linear regression to the application of (9) considering only 4 of the 6 points.

All of the results used to obtain these data can be seen in table 5.

Table 5: Results for the generation of the graph with the relations K and R.

	Angle (θ)	Comp. Angle	SiO_2 (exp)	Si_{2p} (exp)	SiO_2 (∞)	Si_{2p} (∞)	K	R	ln (1+ R/K)	1/sin(θ)
0	5.0	85.0	6974.560	1315.470	5454.482	7728.42100	0.705769	5.301953	2.141513	11.473713
1	15.0	75.0	6163.810	1267.190	4985.648	5224.95800	0.954199	4.864156	1.807901	3.863703
2	25.0	65.0	5272.380	1157.350	4417.939	3490.72900	1.265621	4.555562	1.525941	2.366202
3	35.0	55.0	4714.450	852.420	3249.412	1928.38700	1.685041	5.530666	1.454470	1.743447
4	45.0	45.0	4359.727	558.098	2589.815	455.90530	5.680599	7.811759	0.865067	1.414214
5	55.0	35.0	3501.964	273.184	1375.644	91.13596	15.094415	12.819067	0.614785	1.220775

In the graph, of figure 19, the slope of the linear regression (m) is 0.79. Therefore, by means of (8) and isolating for d, we obtain:

$$d = m\,\lambda \tag{10}$$

$$d = 0.79\,\lambda \tag{11}$$

To obtain the value of λ a wide range of properties for SiO_2 were used such as the number of valence electrons, density and energy bandgap [3] in the program NIST Electron Effective-Attenuation-Length Database [4]. However, these values variate significantly in literature, therefore many of the properties were inserted and an average was made. The λ values obtained can be seen in table 6 with the corresponding parameters. Also given the value of λ it is possible to obtain the thickness of the oxide layer.

Table 6: Parameters to obtain values of λ.

Electron Kinetic Energy (eV)	**Asymmetry Parameter (beta)**	**Valence Electrons**	**Energy Band-gap (eV)**	**Optical Band-gap (eV)**	**Density** (g/cm^3)	λ (Å)	d (Å)
1387.3	1.03	16	8.9	**N.A**	2.27	**35.374**	**28.04**
1387.3	1.03	8	8.9	**N.A**	2.27	**36.7375**	**29.12**
1387.3	1.03	16	8.9	**N.A**	2.65	**33.8105**	**26.80**
1387.3	1.03	8	8.9	**N.A**	2.65	**34.0725**	**27.01**
1387.3	1.03	16	**N.A**	3.85	2.27	**30.39**	**24.09**
1387.3	1.03	8	**N.A**	3.85	2.27	**31.3**	**24.81**
1387.3	1.03	16	**N.A**	3.85	2.65	**29.47**	**23.36**
1387.3	1.03	8	**N.A**	3.85	2.65	**28.7**	**22.75**

Therefore the average thickness obtained is **27.75** Angstroms, with an standard error of 0.533 Angstroms (d = 27.75 ± 0.533 Å) for the energy band-gap. The average thickness obtained for the optical band gap is 23.75 + 0.446 Å. Therefore, by applying a simple average, we obtain a value of 25.6 Å.

This whole procedure was also applied to different samples with distinct conditions. The results can be seen in figure 20, where all the conditions are mentioned and linear regressions to obtain the slope are being determined.

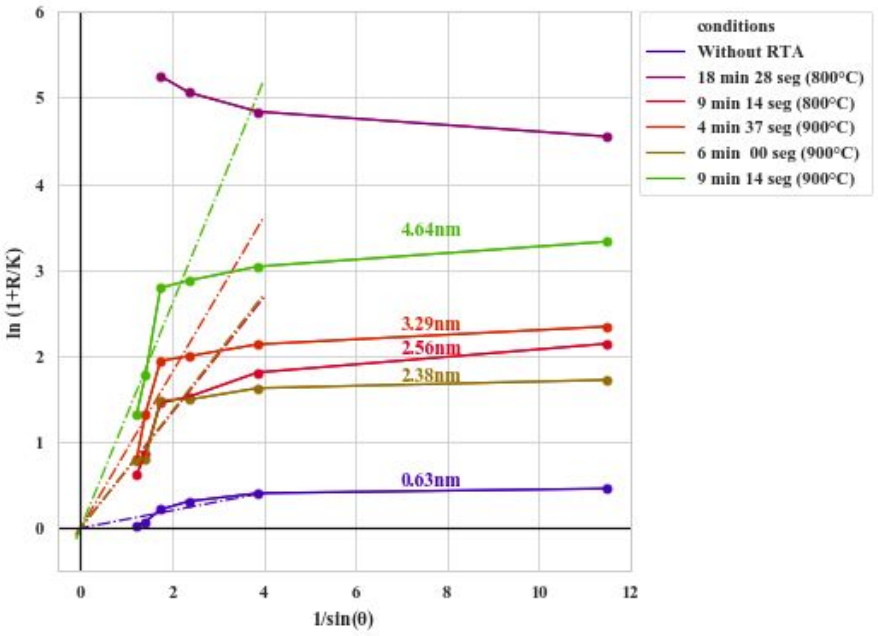

Figure 20: Angular dependent Si2p oxide/ Si2p element ratio data for silicon specimens with 6 different oxide layer thicknesses. Relation to obtain a linear equation for the determination of the thickness of the sample.

In figure 20, it is possible to compare the results with the ones obtained in [2] (see figure 21), where the data is plotted and the patterns seem similar. Linear regressions of the data in the low values from the abscissa axis, show a descent that had to be forced to cero due to physical properties. It is important to mention that in this experiment, the K value was not constant, instead for each experimental point, a different K value was determined, in figure 18 this is not followed exactly, they use a single K value.

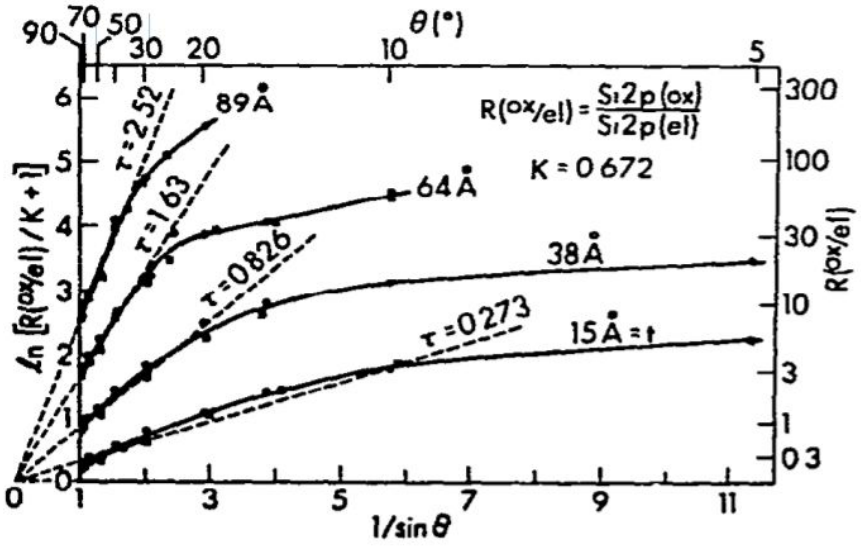

Figure 21: Theoretical data from (2) to show the duality from the procedure.

It is worth noticing that the condition of 18 minutes with 28 seconds at 800°C was not considered for the measurement due to the fact that the values where different compared to the ones obtained from the other conditions, and also due to the fact that the R values are distinct compared to the other sample data (seen in figure 22).

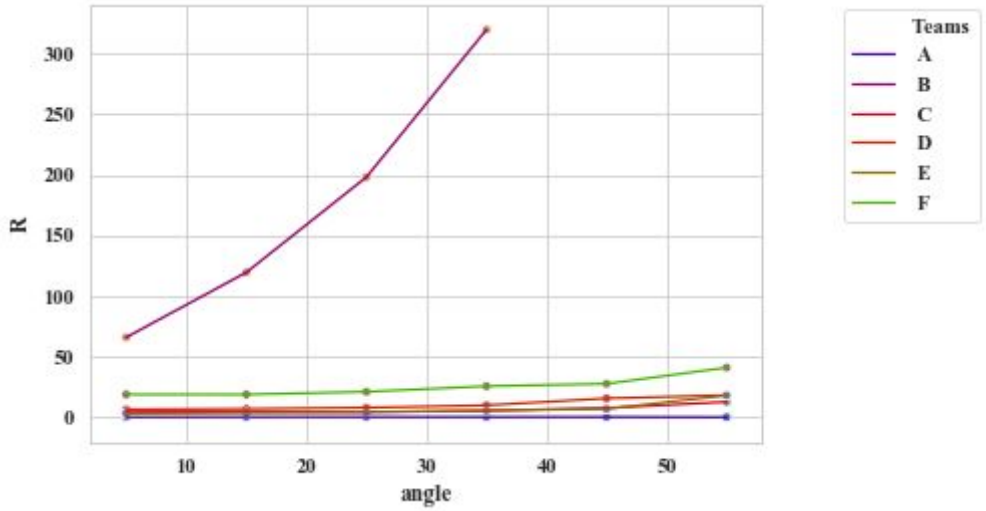

Figure 22. R values for every team.

Conclusions

We obtained the chemical composition that we expected, also we concluded that its behaviour has to be constant because we are measuring the same sample. We, also get a Si semi-oxide, same one that it can be notice in the figure 8, this tell us that our conditions of the oxidation process favored its formation, fact that confirms the success of the RTA process.

With respect to the process of Angular XPS measurements, we conclude it's laborious but also accurate. Reason why it is necessary analyse the data with high precision, in order to get adequate results. Also, this technique has a great potential to work in nano dimensions due to its accuracy and reach.

References

1. Deal and Grove (1965) General Relationship for the Thermal Oxidation of Silicon. Fairchild Semiconductor, a division of Fairchild Camera and Instrument Corporation, Palo Alto, California, USA.

2. Hill et al. (1976) properties of oxidized silicon as determined by angular-dependent x-ray photoelectron spectroscopy. Department of Chemistry, University of Hawaii, Honolulu, Hawaii. USA.

3. Hollauer Ch. (2007) Modeling of thermal Oxidation and Stress Effects. The material Silicon Dioxide. Technischen Universität Wien Fakultät für Elektrotechnik und Informationstechnik von Institute for Mircoelectronics. Online: http://www.iue.tuwien.ac.at/phd/hollauer/node11.html

4. NIST(2011) NIST Electron Effective-Attenuation-Lenght-Database Standard reference Database 82. C. J. Powell, Surface and Microanalysis Science Division National Institute of Standards and Technology Gaithersburg, MD, USA. Retrieved from: https://www.nist.gov/sites/default/files/documents/srd/SRD82UsersGuideV1-3.pdf

https://www.sciencedirect.com/science/article/pii/S092702489700233X